

## Biological Co-Adaptation of Morphological and Composition Traits Contributes to Mechanical Functionality and Skeletal Fragility

Steven M Tommasini,<sup>1</sup> Philip Nasser,<sup>2</sup> Bin Hu,<sup>2</sup> and Karl J Jepsen<sup>2</sup>

**ABSTRACT:** A path analysis was conducted to determine whether functional interactions exist among morphological, compositional, and microstructural traits for young adult human tibias. Data provided evidence that bone traits are co-adapted during ontogeny so that the sets of traits together satisfy physiological loading demands. However, certain sets of traits are expected to perform poorly under extreme load conditions.

**Introduction:** Previous data from inbred mouse strains suggested that biological processes within bone co-adapt morphological and compositional traits during ontogeny to satisfy physiological loading demands. Similar work in young adult humans showed that cortical tissue from slender tibias was stiffer, less ductile, and more susceptible to accumulating damage. Here we tested whether the relationships among morphology and tissue level mechanical properties were the result of biological processes that co-adapt physical traits, similar to those observed for the mouse skeleton.

**Materials and Methods:** Cross-sectional morphology, bone slenderness (Tt.Ar/Le), and tissue level mechanical properties were measured from tibias from 14 female (22–46 yr old) and 17 male (17–46 yr old) donors. Physical bone traits measured included tissue density, ash content, water content, porosity, and the area fractions of osteonal, interstitial, and circumferential lamellar tissues. Bivariate relationships among traits were determined using linear regression analysis. A path analysis was conducted to test the hypothesis that Tt.Ar/Le is functionally related to mineralization (ash content) and the proportion of total area occupied by cortical bone.

**Results:** Ash content correlated negatively with several traits including Tt.Ar/Le and marrow area, indicating that slender bones were constructed of tissue with higher mineralization. Path analysis revealed that slender tibias were compensated by higher mineralization and a greater area fraction of bone.

**Conclusions:** The results suggest that bone adapts by varying the relative amount of cortical bone within the diaphysis and by varying matrix composition. This co-adaptation is expected to lead to a particular set of traits that is sufficiently stiff and strong to support daily loads. However, increases in mineralization result in a more brittle and damageable material that would be expected to perform poorly under extreme load conditions. Therefore, focusing attention on sets of traits and the relationship among traits may advance our understanding of how genetic and environmental factors influence bone fragility.

**J Bone Miner Res** 2008;23:236–246. Published online on October 8, 2007; doi: 10.1359/JBMR.071014

**Key words:** path analysis, biomechanics, stress fracture, sexual dimorphism, functional integration

### INTRODUCTION

THE INCREASED RISK of fracture observed for individuals with slender bones<sup>(1–10)</sup> has generally been attributed to the reduced load-bearing capacity associated with small cross-sectional size or mass.<sup>(11,12)</sup> However, recent studies from our laboratory suggest that variation in tissue quality may also contribute to the increased fracture risk for these individuals. Studies using femora from inbred mouse strains showed that genetic variation in bone slenderness, defined as cross-sectional size relative to length, explained ~50% of

the variation in cortical thickness and tissue mineral density.<sup>(13–15)</sup> We found that slender femora tended to have thicker cortices and higher tissue mineral density, whereas robust femora tended to have thinner cortices and lower tissue mineral density. The correlation between these traits provided evidence that these traits are functionally related (or interacting) in the sense that there are biological processes within bone that work to co-adapt morphological and tissue quality traits during ontogeny.<sup>(16–21)</sup> The term functional interaction is used because presumably these biological processes ensure that the set of traits is sufficiently stiff and strong for daily loads.<sup>(22–24)</sup>

A downside of these biological processes is that not all

The authors state that they have no conflicts of interest.

<sup>1</sup>New York Center for Biomedical Engineering, CUNY Graduate School, Department of Biomedical Engineering, City College of New York, New York, New York, USA; <sup>2</sup>Leni & Peter W. May Department of Orthopaedics, Mount Sinai School of Medicine, New York, New York, USA.

sets of traits result in equivalent failure mechanisms. For slender bones, the compensatory increases in cortical thickness and tissue mineral density may help to increase organ level stiffness, but the reduced tissue ductility and toughness associated with the greater tissue mineral density<sup>(25)</sup> may increase the risk of fracturing under extreme loading conditions, such as low cycle fatigue (e.g., military training) and overloading (e.g., falling). Previous data suggested that the human skeleton may possess biological processes that co-adapt traits,<sup>(16,21,26)</sup> similar to those observed for the mouse skeleton. Cortical tissue from slender tibias of young adult males and females was stiffer, less ductile, and more susceptible to accumulating damage compared with tissue from more robust tibias.<sup>(27,28)</sup> Thus, the biological processes that co-adapt traits to accommodate variable bone size or mass may also contribute to increased fracture risk.

The goal of this study was to test whether morphological and tissue quality traits are functionally related, because this would imply there is a strong biological process in bone that co-adapts traits. We hypothesize that the morphological traits will co-vary with matrix composition and/or architectural traits that contribute to bone stiffness and strength. For slender bones, we postulate that the small cross-sectional size is compensated by higher mineralization and a proportionally greater amount of cortex. We tested this hypothesis by conducting a path analysis to determine whether there are functional interactions among morphological and tissue quality traits for young adult human tibias.

## MATERIALS AND METHODS

### *Sample population*

Tibias of 14 female donors (12 white, 1 black, and 1 unknown) 22–46 yr of age (average age =  $36.9 \pm 8.1$  yr) and 17 male donors (15 white, 1 Hispanic, and 1 black) 17 to 46 yr (average age =  $32.9 \pm 10.4$  yr) were acquired from the Musculoskeletal Transplant Foundation (Edison, NJ, USA) and the National Disease Research Interchange (Philadelphia, PA, USA). The morphologic and tissue level mechanical property data used in this analysis were reported in previous studies.<sup>(27,28)</sup> Donor body weight and height were obtained from the source. Only tibias from donors with no known skeletal pathology were included in the study. Tibias were freshly harvested, wrapped in wet gauze, and stored in plastic bags at  $-40^{\circ}\text{C}$ .

### *Bone morphology*

As described previously,<sup>(27,28)</sup> each tibia was assessed for global measures of morphology, including measures of tibia length (Le)<sup>(29)</sup> and the mid-diaphyseal bone diameters in the anteroposterior ( $B.Dm_{AP}$ ) and mediolateral ( $B.Dm_{ML}$ ) directions. Cross-sectional morphological traits were quantified from 3-mm-thick diaphyseal cross-sections cut at 30%, 50%, and 70% of the total tibia length. These morphological traits included cortical area (Ct.Ar), total area (Tt.Ar), marrow area (Ma.Ar), polar moment of inertia (J), and cortical thickness (Ct.Th). All morphological traits were averaged over the three cross-sections for each tibia.

Because the cross-section of the tibia has a nonuniform cortical thickness, the average cortical thickness was determined as  $2 \times \text{Ct.Ar}/(\text{P.Pm} + \text{E.Pm})$ , where P.Pm and E.Pm are the periosteal and endosteal perimeters, respectively. Slenderness was defined as the ratio of total area to tibia length ( $\text{Tt.Ar}/\text{Le}$ ). The ratio of internal diameter to external diameter (K) has been examined previously in the context of identifying the optimal value of K that allows for minimal mass and maximal stiffness for hollow structures like long bone diaphyses.<sup>(30)</sup> In this study, we tested how K varied with sex and slenderness for human tibias. Because the nonuniform shape of the tibia diaphysis precludes measuring a single diameter directly, an estimate of the internal and external diameters was calculated for each cross-section from Ma.Ar and Tt.Ar, respectively, assuming a circular cross-section.  $\text{Ct.Ar}/\text{Tt.Ar}$  correlated negatively with K ( $R = -0.99$ ,  $p = 0.001$ ), as expected, indicating that the estimated internal and external diameters provided a reasonable approximation of K for the nonuniform tibia cross-sections.

### *Tissue level mechanical properties*

Cortical bone samples were prepared for biomechanical testing as described previously.<sup>(27,28)</sup> A total of eight samples were generated from each tibia and randomly distributed to monotonic ( $n = 4$ ) and damage accumulation ( $n = 4$ ) test groups. All samples were stored at  $-40^{\circ}\text{C}$  in gauze saturated with PBS with added calcium<sup>(31)</sup> and placed individually in airtight bags. Tissue level monotonic properties were assessed by loading four cortical bone samples from each tibia to failure in four-point bending at 0.05mm/s using a servohydraulic materials testing system (Instron model 8872; Instron Corp., Canton, MA, USA). Specimens were submerged in a PBS solution with 57.5mg/liter of calcium added<sup>(31)</sup> and maintained at  $37^{\circ}\text{C}$  throughout all tests. Load and deflection were converted to stress and strain as described previously.<sup>(27)</sup> These bending equations take yielding into consideration,<sup>(32)</sup> and thus provide an estimate of tissue strength that is consistent with tensile mechanical properties.<sup>(33)</sup> Tissue modulus, strength, post-yield strain, and energy-to-fracture (toughness) were calculated from the stress-strain curve. All properties were averaged over the four samples tested for each tibia. Tissue damageability was assessed for four cortical bone samples per tibia using a protocol that was designed to induce and accumulate cracks in cortical bone specimens and to measure the degradation of stiffness as a surrogate measure of damage accumulation.<sup>(27,28,34)</sup> For each diagnostic cycle,  $i$ , stiffness ( $S_i$ ) was calculated from a linear regression of the initial portion of the load deformation curve. The total amount of damage induced in each sample was calculated by comparing the stiffness (N/mm) values measured at the end of the entire test sequence (postdamage diagnostic cycles) to the values measured during the initial (predamage) cycles.

### *Tissue microstructure*

To test for variation in matrix organization, bone microstructure was assessed for each sample retrieved from the damageability tests ( $n = 4/\text{tibia}$ ). Samples were fixed, bulk-

stained in basic fuchsin, dehydrated, and embedded undecalcified in poly-methylmethacrylate. For each sample, digital images of three transverse sections, 100  $\mu\text{m}$  in thickness, were taken at  $\times 10$  magnification, stitched together, and traced using an interactive tablet monitor (Wacom Company, Tokyo, Japan). Parameters measured included porosity and the area fractions of osteonal, interstitial (remodeled), and circumferential lamellar (unremodeled) tissues. Both vascular canals and resorption spaces were counted as pores. Osteonal tissue was defined as a lamellar region with a haversian canal completely surrounded by a cement line. Data from individual test samples were averaged for each donor.

### Tissue composition

Variation in tissue mineral density was assessed by measuring the density, ash content, and water content for each sample retrieved from the monotonic tests ( $n = 4/\text{tibia}$ ). Samples were defatted using a 1:1 volume ratio of ethanol/ether for 8 h followed by a 2:1 volume ratio of chloroform/methanol for 8 h. The methanol residue was removed by using two changes of pure chloroform for 1 h each. Samples were rehydrated, degassed in distilled water in a 25-mm Hg vacuum for 4 h, and allowed to stand at atmospheric conditions for an additional hour. Sample volume was determined using Archimedes principle by measuring the weight while the sample was suspended from a fine wire in distilled water (submerged weight). Samples were placed in a centrifuge for 10 min at 8000g with the cap of the vial closed to control humidity and immediately weighed to obtain the hydrated weight. Samples were dried under vacuum at 80°C for 24 h to constant weight and reweighed (dry weight). Finally, samples were ashed at 600°C for 18 h, reweighed (ash weight), degassed under vacuum for 2 h, and reweighed while suspended from a fine wire in distilled water (submerged ash weight). Density was calculated as (hydrated weight)/(sample volume), where sample volume = hydrated weight – submerged weight. Ash content was calculated as the ash weight normalized by the hydrated weight. Water content was calculated as (hydrated weight – dry weight)/(hydrated weight).

### Statistical analysis

Pearson correlation coefficients were calculated to test whether the morphologic traits and the tissue level mechanical properties correlated significantly with the matrix architectural and compositional traits. Differences in physical traits between males and females were determined using a Student's *t*-test. The data were not corrected for age or body weight for either test.

### Path analysis

To test the hypothesis that morphological and tissue quality traits are functionally related, a path analysis was conducted because this allows for testing how multiple traits co-vary simultaneously.<sup>(35)</sup> Path models were constructed by specifying the directed paths among select bone traits. Directed paths identify related traits and indicate the direction of the relationship between them. The focus of

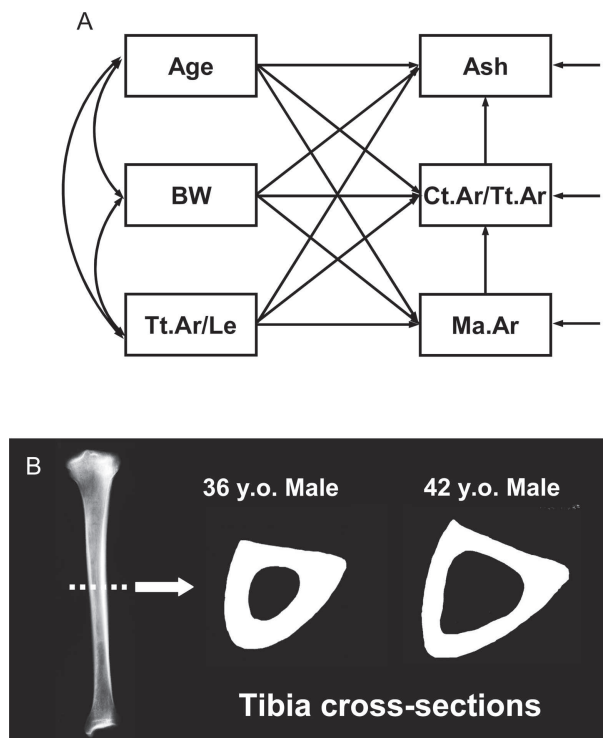


**FIG. 1.** Schematic drawing of (A) the proposed path analysis showing all possible combinations of connections and (B) diaphyseal cross-sections showing the variation in size for slender (left) and robust (right) tibias.

this analysis is the interaction of traits and not how traits define global function. Traits were selected to test for associations between bone morphology and tissue quality parameters. We focused on ash content given our prior work in inbred mouse strains, which showed that co-variation among adult morphology and mineralization arise during postnatal growth.<sup>(15,36)</sup> Therefore, finding an association between slenderness and ash content in the human skeleton would suggest that biological processes observed in the mouse also exist in the human skeleton. For the path model (Fig. 1A), we postulated that relationships occur in a particular order in which slender bones (Tt.Ar/Le) are compensated by higher mineralization (ash content) and a proportionally greater amount of cortical bone. Because slender tibias tend to have a similar cortical thickness as more robust tibias (Fig. 1B), incorporating traits like Ct.Th or Ct.Ar into the model would not be expected to differentiate individuals with more/less bone. Rather, we used the ratio, Ct.Ar/Tt.Ar, because this trait can be related to the relative amount of tissue, and it can be related to the relative expansions of the periosteal and endosteal surfaces during ontogeny. Ct.Ar/Tt.Ar also was used rather than K because the relative amount of cortical tissue can be more easily related to whole bone stiffness than the relative amount of marrow space. An arrow was also included between Ct.Ar/Tt.Ar and ash content to take into consideration the variance in ash content that was not accounted for by slenderness. Data for males and females were analyzed separately to account for the influence of dimorphic growth

patterns. The generalized model (Fig. 1A) was modified for each sex by specifying the minimum number of connected traits that best explained the variance in ash content and Ct.Ar/Tt.Ar.

Path coefficients, which represent the magnitude of the direct and indirect relationships between traits, were calculated using the standardized (Z-transformed) data (LISREL v.8.8; Scientific Software International, Lincolnwood, IL, USA). Male and female data were converted to Z-scores separately to eliminate size effects. Structural equations were constructed using the path coefficients to specify the interconnected relationships. Observed and model-implied covariance matrices were compared using maximum likelihood estimation, and overall fit was determined by a  $\chi^2$  test. Unlike conventional null hypothesis testing, path analysis favors the a priori, theory-based model such that models are only rejected if the observed data and the expectations derived from the model do not match (i.e., if  $p < 0.05$ ).<sup>(37)</sup> Thus,  $\chi^2$  values with an associated  $p > 0.05$  indicate that the model adequately fits the data. The root mean square error of approximation (RMSEA) was also reported as an additional fit index. RMSEA is a measure of fit adjusted for population size and takes the number of degrees of freedom of the model into consideration.<sup>(38,39)</sup> For RMSEA, the  $p$  value represents the significance of fit with  $p < 0.05$  indicating close fit,  $0.05 < p < 0.08$  indicating fair fit, and  $p > 0.10$  indicating poor fit.<sup>(39)</sup> Path analysis as used here is similar to multivariate analysis in how the structural equations are developed. However, conventional multivariate methods seek to estimate generic fixed models (e.g., canonical correlation) and lack the flexibility required to represent the model that best matches a particular situation (i.e., directed relationships).<sup>(37)</sup> Thus, path analysis allowed us to test whether specific relationships among morphological and compositional traits exist for human tibias.

## RESULTS

### *Tissue microstructure and composition*

Although the tissue density and porosity of cortical tissue were similar for females and males, females showed a 1.3% greater ash content compared with males ( $p < 0.02$ ,  $t$ -test), a 4.5% lower water content ( $p < 0.06$ ,  $t$ -test), and a 43% greater area fraction of unremodeled tissue ( $p < 0.01$ ,  $t$ -test) compared with males (Table 1). Total porosity increased with age for males ( $p < 0.005$ ), but this relationship was only borderline significant for females ( $p < 0.08$ ; data not shown). Ash content increased with age for males ( $p < 0.03$ ) but not females ( $p < 0.6$ ; data not shown).

### *Correlation between tissue level mechanical properties and tissue quality*

Because the relationships among the tissue level mechanical properties and the compositional and architectural traits were similar for males and females, the datasets were combined for the correlation analysis. Significant correlations were observed between the tissue level mechanical properties and several of the matrix compositional and mi-

TABLE 1. PHYSICAL BONE TRAITS FOR CORTICAL TISSUE OBTAINED FROM THE TIBIAS OF YOUNG ADULT FEMALES AND MALES

<i>Trait</i>	<i>Females (n = 14)</i>	<i>Males (n = 17)</i>	<i>t-test, p value</i>
Density (g/ml)	2.05 ± 0.04	2.03 ± 0.04	0.37
Ash content (%)	61.8 ± 1.1	61.0 ± 0.6	0.02
Water content (%)	11.2 ± 0.7	11.7 ± 0.7	0.06
Total porosity (%)	4.7 ± 1.7	5.4 ± 1.7	0.27
Osteonal tissue (%)	72.2 ± 5.0	71.4 ± 5.3	0.66
Unremodeled tissue (%)	13.2 ± 6.6	7.5 ± 5.0	0.01

Significant difference between males and females for  $p < 0.05$ .

crostructural traits, as expected (Table 2). Tissue modulus (Fig. 2A) and strength both increased with ash content, whereas postyield strain (Fig. 2B) and toughness decreased. Modulus, strength (Fig. 2C), toughness, and postyield strain all decreased with increasing porosity, whereas the damage parameter increased (Fig. 2D). The area fraction of osteonal tissue and unremodeled tissue showed no significant correlations with any of the tissue level mechanical properties.

### *Correlation between bone morphology and tissue quality*

Linear regression analyses conducted using uncorrected data showed significant correlations between several bone morphological traits and measures of tissue composition and microstructure (Table 3). Ash content correlated negatively with several traits including Tt.Ar/Le (a measure of bone slenderness; Fig. 3A) and Ma.Ar (Fig. 3B), indicating that slender bones (low Tt.Ar/Le and Ma.Ar) were constructed of tissue with a higher degree of mineralization. Total porosity correlated negatively with Ct.Ar/Tt.Ar and positively with K, indicating that tibias with a proportionally larger amount of cortex relative to overall bone size showed a reduced amount of porosity. K was similar ( $p < 0.88$ ,  $t$ -test) for males ( $0.61 \pm 0.04$ ) and females ( $0.61 \pm 0.03$ ), and the overall range was 0.56–0.70. The amount of unremodeled tissue decreased with Tt.Ar/Le, indicating that smaller bones tended to have more unremodeled tissue.

### *Path analysis*

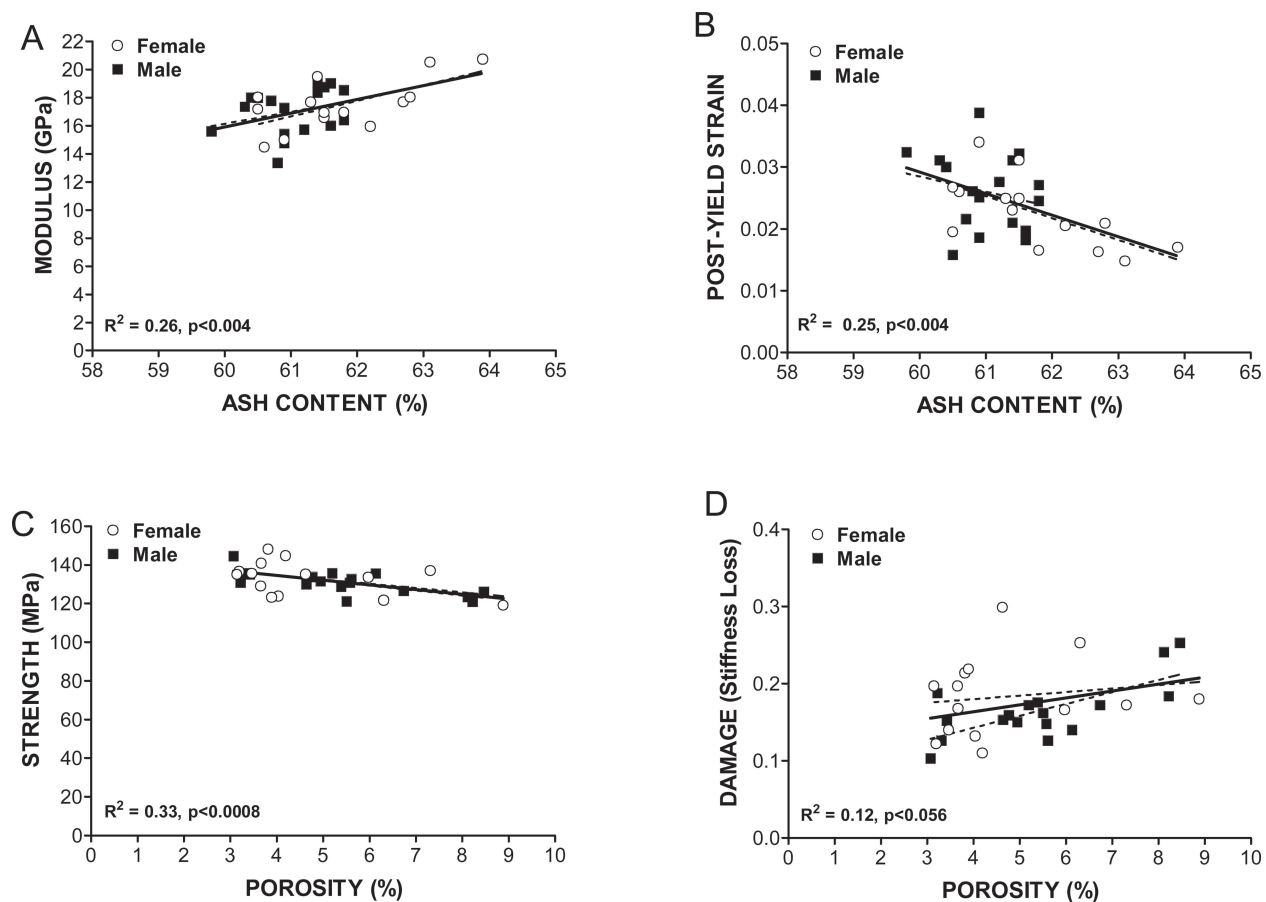
Path analysis was conducted to test whether the tissue quality traits were functionally related to the morphological traits. For males, the final path model included all traits from the generalized model (Fig. 1A) but with four fewer connections (Fig. 4A). The  $\chi^2$  ( $\chi^2 = 4.2$ ,  $p < 0.52$ ) and RMSEA ( $p = 0.00$ ) values both indicated that there was an excellent fit between the data and the path model. The large path coefficients between body weight and Ma.Ar and between age and ash content indicated that body weight and age were important covariates for the males. Holding these covariates fixed revealed that bone slenderness (Tt.Ar/Le) was functionally related to ash content and the relative amount of cortical tissue (Ct.Ar/Tt.Ar). The path coefficients were calculated based on Z-transformed data and thus reflect the number of SD changes in a trait arising



TABLE 2. PEARSON CORRELATION COEFFICIENTS RELATING TISSUE MICROSTRUCTURE AND COMPOSITION WITH TISSUE LEVEL MECHANICAL PROPERTIES (COMBINED MALES AND FEMALES)

	<i>Modulus</i>	<i>Strength</i>	<i>PY strain</i>	<i>Toughness</i>	<i>Damage (S)</i>
Tissue density	0.18 (0.34)	0.10 (0.58)	-0.01 (0.95)	0.02 (0.92)	<b>0.37</b> <b>(0.04)</b>
Ash content	<b>0.51</b> <b>(0.004)</b>	0.30 (0.10)	<b>-0.50</b> <b>(0.004)</b>	<b>-0.35</b> <b>(0.05)</b>	0.21 (0.27)
Water content	0.26 (0.16)	-0.05 (0.80)	0.01 (0.95)	-0.03 (0.88)	-0.07 (0.72)
Total porosity	-0.17 (0.35)	<b>-0.57</b> <b>(0.001)</b>	-0.23 (0.21)	-0.33 (0.07)	0.35 (0.06)
Osteonal tissue	0.17 (0.38)	-0.17 (0.35)	-0.02 (0.91)	-0.04 (0.84)	0.28 (0.12)
Unremodeled tissue	-0.03 (0.86)	0.13 (0.50)	-0.10 (0.61)	-0.06 (0.76)	-0.09 (0.65)

*p* values shown in parentheses. Bold entries denote significant relationships ( $p < 0.05$ ).



**FIG. 2.** Significant correlations were observed among tissue level mechanical properties and matrix compositional and microstructural traits. Linear regressions are shown for (A) tissue modulus vs. ash content, (B) postyield strain vs. ash content, (C) strength vs. porosity, and (D) the damage parameter vs. porosity. The thick, solid line represents the regression for the combined male and female dataset.

from a 1 SD change in slenderness. The path coefficients among the morphological traits were large, as expected. When all direct and indirect paths were taken into consideration, a 1 SD decrease in Tt.Ar/Le was associated with a 0.76 SD increase in Ct.Ar/Tt.Ar. This indicated that more slender bones tended to have a cortex that occupied pro-

portionally more space. This path model accounted for 65% of the variation in Ma.Ar and 92% of the variation in Ct.Ar/Tt.Ar. Furthermore, there was a large path coefficient between Ct.Ar/Tt.Ar and ash content. Although the direct path between slenderness and ash content showed a weak coefficient of -0.13, when the indirect paths through

TABLE 3. PEARSON CORRELATION COEFFICIENTS RELATING TISSUE MICROSTRUCTURE AND COMPOSITION WITH PHYSICAL BONE TRAITS (COMBINED MALE AND FEMALE DATASETS)

	<i>Tt.Ar</i>	<i>Ct.Ar</i>	<i>Ma.Ar</i>	<i>Tt.Ar/Le</i>	<i>Ct.Ar/Tt.Ar</i>	<i>K</i>	<i>I<sub>AP</sub></i>	<i>I<sub>AP</sub>/(B.Dm<sub>AP</sub>/2)</i>
Tissue density	-0.21 (0.26)	-0.24 (0.20)	-0.14 (0.45)	-0.16 (0.40)	-0.07 (0.71)	0.06 (0.75)	-0.25 (0.18)	-0.26 (0.17)
Ash content	<b>-0.43</b> <b>(0.02)</b>	<b>-0.38</b> <b>(0.03)</b>	<b>-0.42</b> <b>(0.02)</b>	<b>-0.36</b> <b>(0.05)</b>	0.17 (0.37)	-0.17 (0.38)	<b>-0.37</b> <b>(0.04)</b>	<b>-0.38</b> <b>(0.04)</b>
Water content	0.20 (0.29)	0.25 (0.17)	0.09 (0.63)	0.14 (0.47)	0.10 (0.59)	-0.10 (0.60)	0.24 (0.20)	0.21 (0.26)
Total porosity	0.23 (0.22)	0.10 (0.58)	<b>0.37</b> <b>(0.04)</b>	0.29 (0.11)	<b>-0.46</b> <b>(0.01)</b>	<b>0.45</b> <b>(0.01)</b>	0.20 (0.17)	0.14 (0.45)
Osteonal tissue	0.04 (0.82)	-0.06 (0.73)	0.18 (0.33)	0.06 (0.74)	-0.32 (0.08)	0.31 (0.09)	0.04 (0.85)	-0.02 (0.91)
Unremodeled tissue	<b>-0.38</b> <b>(0.03)</b>	-0.29 (0.11)	<b>-0.45</b> <b>(0.01)</b>	<b>-0.40</b> <b>(0.03)</b>	0.33 (0.08)	-0.33 (0.07)	-0.33 (0.07)	-0.29 (0.11)

*p* values shown in parentheses. Bold entries denote significant relationships ( $p < 0.05$ ).

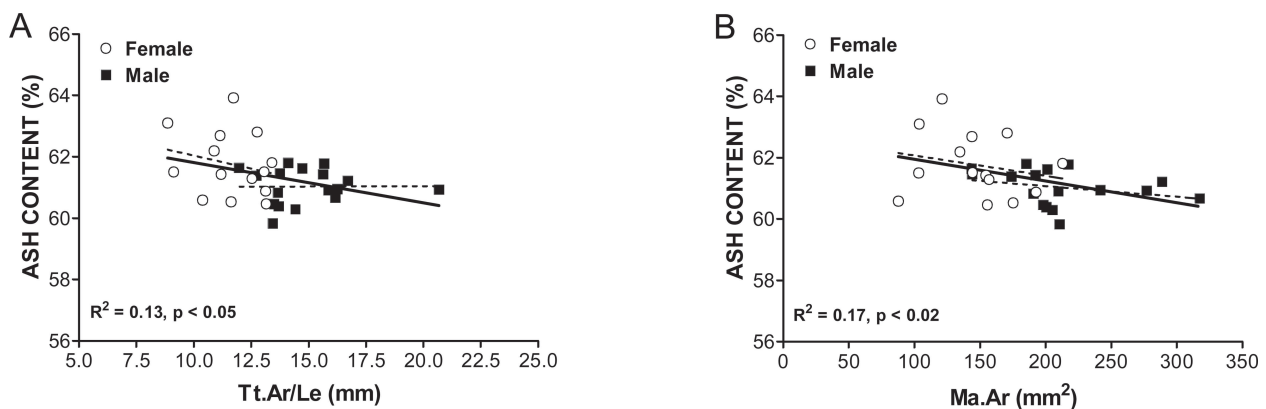


FIG. 3. Relationships between bone morphology and matrix compositional and microstructural traits. Linear regressions are shown for (A) ash content vs. *Tt.Ar/Le* (slenderness) and (B) ash content vs. marrow area. The thick, solid line represents the regression for the combined male and female dataset.

*Ct.Ar/Tt.Ar* and *Ma.Ar* were considered, the relationship between slenderness and ash content was negative, with an overall path coefficient of  $-0.41$ . Using this path model, 48% of the variation in ash content among the males was explained based on bone morphology. The path model thus indicated that slender male tibias were compensated by a higher degree of mineralization and a proportionally greater amount of cortex.

For females, the general path model (Fig. 1A) was modified substantially to arrive at a model that adequately fit the data. The final path model for females (Fig. 4B) was different than the males. Body weight had only a minor influence on the relationships among traits, and consequently, this variable was removed from the path model. The path coefficients among *Tt.Ar/Le*, *Ma.Ar*, and *Ct.Ar/Tt.Ar* were large and accounted for 63–90% of the variation in *Ma.Ar* and *Ct.Ar/Tt.Ar*, similar to that observed for the males. Unlike the males, a connection between *Ma.Ar* and ash content was required for the female data, and the path coefficient was quite large ( $-1.76$ ). When the path model for the males was run with this connection, the path coefficient between *Ma.Ar* and ash content was only 0.07, and there was a decrease in the overall fit of the model. This

indicated that this path was unique for the female data. This model explained 22% of the variation in ash content among the females, which was only one half of that explained for the males. Nevertheless, when age was held constant, a 1 SD decrease in *Tt.Ar/Le* was associated with a 0.23 SD increase in ash content and a 0.30 SD increase in *Ct.Ar/Tt.Ar*. Thus, like the males, slender female tibias were also associated with a higher degree of mineralization and a proportionally greater amount of cortical bone.

The path analysis was repeated by replacing *Ct.Ar/Tt.Ar* with *K*. This analysis resulted in nearly identical path coefficients and had the same explanatory power for ash content. The only difference was the path coefficients immediately connecting with *K* were opposite in sign to those determined for *Ct.Ar/Tt.Ar*, as expected (data not shown).

## DISCUSSION

### *Morphological and tissue quality traits are functionally related*

The bivariate analysis confirmed the hypothesis that morphological traits correlate or co-vary with matrix com-

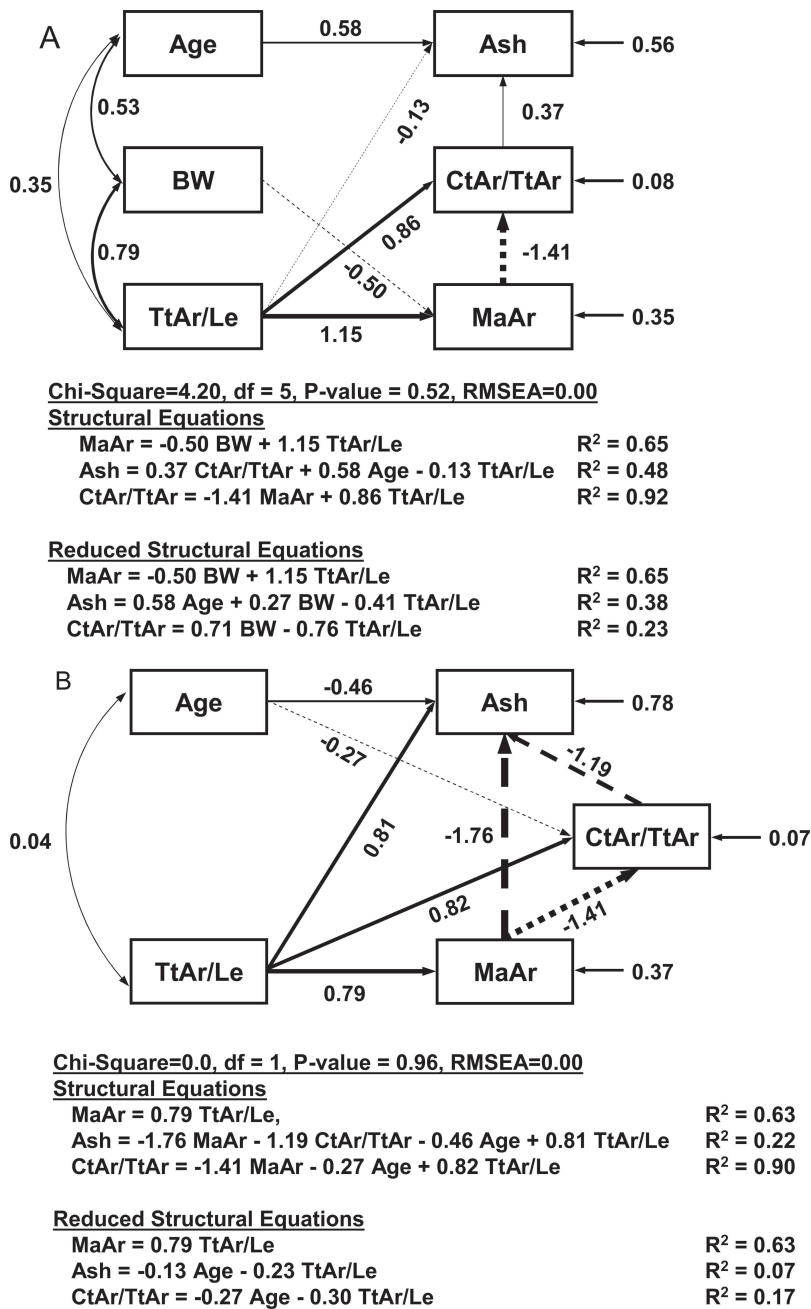


**FIG. 4.** Path analysis (with least number of variables and connections) showing traits, connections between traits, and path coefficients for (A) males and (B) females.

positional and microstructural traits in the human skeleton. The path analysis further revealed that the relationship between bone slenderness and ash content observed in the bivariate correlation analysis was actually part of a larger association that involved the relative size of the marrow space and thus the proportion of the diaphysis that was occupied by cortical tissue (i.e., the inverse of K). These associations were independent of body weight, age, and sex. Path analysis, which is based on conditional covariances,<sup>(35)</sup> provides a rigorous statistical approach to reveal relationships among physical bone traits when co-factors such as age and body size can obscure these relationships. Age and body size were easily corrected in this study because the

physical traits (e.g., Tt.Ar, Ct.Ar, ash content, porosity) varied linearly with each co-factor for this young-adult population (data not shown).

The functional relationships between bone morphology and mineralization observed in this study are consistent with prior work comparing various bones subjected to radically different mechanical loading environments from different species.<sup>(17)</sup> These functional interactions have also been reported for long bones and vertebrae from genetically distinct inbred mouse strains,<sup>(15,40)</sup> phalangeal segments from the brown bat,<sup>(20)</sup> and during long bone growth.<sup>(41–43)</sup> Our path model focused primarily on ash content<sup>(13)</sup> as a measure of matrix composition, because

this particular trait is an important determinant of tissue level stiffness and ductility. However, it is entirely possible that variation in tissue stiffness could arise by variation in other matrix components, such as collagen architecture and porosity,<sup>(44,45)</sup> and these factors could be incorporated into similar path models. When body size and age were taken into consideration, slender tibias were also found to have less porosity and a greater area fraction of unremodeled tissue compared with more robust tibias. The negative correlation between bone slenderness and the area fraction of unremodeled tissue is consistent with Ural and Vashishth,<sup>(46)</sup> who examined bone samples over a much larger age range and showed that slender tibias contain a greater amount of interstitial tissue compared with more robust tibias. A lower amount of remodeling may partly explain the increase in ash content in smaller bones. Because ash content is a tissue averaged measure of the amount of mineral packed into the matrix, further examination using backscatter electron (BSE) or FTIR imaging is needed to more comprehensively assess the heterogeneity of tissue mineral content, its association with organic matrix constituents, and its contribution to material stiffness.

*Functional interactions among traits provide new insight into biological control mechanisms in bone*

Our prior work reported significant correlations between bone morphology and tissue level mechanical properties, including measures of stiffness and ductility.<sup>(27,28)</sup> The results of the path analysis showed that these associations arise in part because of variation in matrix composition. Path analysis differs from multiple regression analysis in many ways,<sup>(37)</sup> but one important aspect here is that connections among traits are specified in a particular way to reveal order and thus should be traceable to a biological mechanism. Although the biological nature of co-adapted traits in bone is not fully understood, finding that morphological and compositional traits were functionally related provides further evidence that biological controls exist in bone whereby mechanical functionality is established during ontogeny by adapting a set of traits so together they satisfy physiological loading demands.<sup>(42)</sup> For long bones, the set of traits are expected to result in a structure that is sufficiently stiff for daily loading demands.<sup>(22–24)</sup> Transgenic mouse strains provided evidence that alterations in an extracellular matrix protein can elicit adaptive responses to possibly compensate for the changes in tissue quality.<sup>(47)</sup> Although the mouse and human skeletons differ in scale and microstructure, the basic concept that traits are co-adapted to create a mechanically functional structure seems to translate from the mouse to the human skeleton.

The generalized path model (Fig. 1A) was constructed based largely on a priori knowledge of how biological processes define bone size and shape during growth for the human<sup>(48)</sup> and mouse skeletons.<sup>(15,36)</sup> Thus, the functional interactions among traits observed in the adult skeleton are a manifestation of biological processes that exist during ontogeny. We expect that the biological mechanism(s) responsible for these functional interactions will be determined by additional research examining skeletal growth patterns.<sup>(36)</sup>

Variation in size and shape among individuals reflects the various genetic and environmental factors that promote or inhibit periosteal expansion relative to longitudinal growth. If bone did not possess biological processes to co-adapt traits, there would be little chance of observing any consistent relationship among traits for the unrelated individuals examined in this study. Thus, these data suggest that these individuals share common biological controls during ontogeny. Although it is not entirely clear how co-adapted traits arise, one theory suggests that co-adapted traits are a consequence of genes affecting hormonal regulation, which have pleiotropic effects.<sup>(49)</sup> It is expected that having the biological processes to co-adapt skeletal traits was fixed in the genome during evolution, because these processes would be expected to increase fitness and survival by allowing for multiple ways to grow structures that match daily loading demands.<sup>(16,26)</sup> This would have the effect of dampening the deleterious effects of the environmental<sup>(49)</sup> and genetic<sup>(35)</sup> factors that promote a slender bone phenotype. The biological paradigm that traits are co-adapted is not limited to bone but has also been observed for the heart.<sup>(50)</sup>

*Interactions among physical traits contribute to mechanically functional structures*

The data provide important new insight into how mechanically functional structures are constructed. The results suggested that bone adapts in at least two ways. First, the negative association between Tt.Ar/Le and Ct.Ar/Tt.Ar suggests that bone adapts by varying the relative amount of cortical bone within the diaphysis. This negative correlation indicates that marrow size is proportionally smaller in slender bones compared with robust bones. The relationship between external and internal diameters (K) has been examined previously in the context of identifying the optimal value of K that allows for minimal mass and maximal stiffness for a hollow structure.<sup>(30)</sup> Prior work compared inter- and intraspecies effects, but there are no data on how K varies with bone slenderness. For slender bones, adapting by reducing marrow size (lower K) would maximize the amount of bone within the diaphysis to increase overall stiffness. For robust bones, this adaptive response would minimize the amount of bone to reduce overall mass. This adaptive process would require that the relative expansion rates of the endosteal and periosteal surfaces are coupled and thus biologically controlled during ontogeny.<sup>(36)</sup>

Second, the negative association between Tt.Ar/Le and ash content suggests that bone also adapts by varying matrix composition. This negative correlation is consistent with the idea that increasing the amount of mineral incorporated within the matrix will result in a compensatory increase in tissue stiffness that could partly compensate for the reduced cross-sectional size of a slender long bone. This adaptive mechanism would require that osteoblasts, or possibly osteocytes, sense their environment and modulate matrix composition. The biological control mechanisms that regulate mineral content are not fully understood, but it is clear that matrix mineralization varies among bones with different functions.<sup>(17)</sup> The association between slenderness



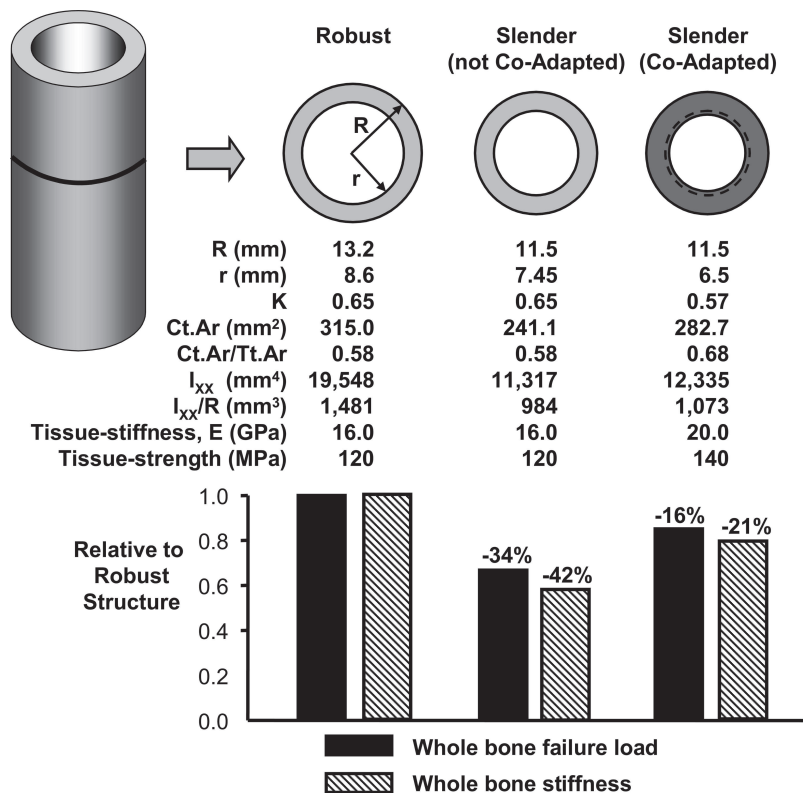


**FIG. 5.** Schematic illustration of how co-adaptation of morphological and compositional traits acts to increase overall stiffness and failure load of a slender cylindrical structure. The slender structure, without co-adapted traits, has the same tissue-modulus (E), K, and Ct.Ar/Tt.Ar as the robust structure, but this results in a dramatically lower stiffness and failure load. The slender structure with co-adapted traits has a slightly smaller marrow area (lower K, higher Ct.Ar/Tt.Ar) and larger tissue-modulus and tissue strength compared with the robust structure. These small changes increase the stiffness and failure load of the slender bone so that they are closer to the robust structure.

and mineralization may act to further increase global stiffness and strength beyond that which can be accommodated by morphological variation. This is particularly important because addition of bone to the endosteal surface, although useful, presents a limitation to how much compensation can occur solely on a morphological basis. Thus, matrix level adaptations may be needed to further increase global stiffness and strength.

As shown in Fig. 5, the two adaptive processes have an important effect on whole bone stiffness and strength. Whole bone stiffness under bending loads is proportional to the tissue modulus (E) times the rectangular moment of inertia (I) and failure load is proportional to tissue strength times section modulus (I/R). If biological processes did not co-adapt traits, a slender bone with the same length, K, and mineral content (and thus tissue modulus and tissue strength) as a robust bone would have ~30–40% reductions in whole bone stiffness and failure load and would likely be underdesigned for normal daily loading conditions. For slender bones, relatively subtle increases in endosteal bone and mineral content (tissue modulus), consistent with the current dataset and indicative of biological processes that co-adapt traits, have the benefit of increasing overall stiffness and failure load closer to that of the robust bone. Furthermore, co-adaptation of traits in slender bones does not result in greater cortical area relative to body weight compared with robust bones. Consequently, there does not seem to be a metabolic cost associated with this co-adaptation.

#### *Interactions among physical traits contribute to increased risk of stress fractures*

We studied the tibia diaphysis from young adult males and females because bone slenderness in this age group is correlated with increased risk of stress fractures in athletes<sup>(7)</sup> and military recruits.<sup>(11,12)</sup> Individuals with slender bones, which are measured clinically as diaphyses with a small cross-sectional size for a given length and metaphyses with lower bone mass, show low BMD and a higher fracture incidence throughout life compared with individuals with robust bones.<sup>(5–8,11,12,51,52)</sup> The increased fracture risk of slender bones has typically been attributed to the reduced load carrying capacity associated with the small cross-sectional size and mass.<sup>(8,11)</sup> However, the current data may provide new insight into this problem. Our data showed that slender bones were compensated by increased ash content and a proportionally greater amount of cortical tissue. Although this co-adaptation has the benefit of ensuring a particular set of traits is sufficiently stiff and strong to support daily loads, the downside is that not all sets of traits result in equivalent failure mechanisms. For slender bones, the combination of a thicker cortex and higher mineral content may help to increase organ level stiffness, but the reduced tissue ductility and toughness that were associated with the greater ash content may increase the risk of fracturing under extreme loading conditions, such as low cycle fatigue (e.g., military training) and overload (e.g., falling). Thus, this co-adaptation, because it involves matrix miner-

alization, seems to result in the development of preferred sets of adult traits within the context of extreme load conditions.

*Sexual dimorphism contributes to differences in functional interactions among bone traits*

Studying young adults allowed us to test for relationships among physical bone traits at the end of the growth phase and before appreciable bone loss begins. Males and females showed similar relationships between matrix composition, microstructure, and tissue level mechanical properties. This indicates that, at least at this level of analysis, males and females construct bone material in a similar way.<sup>(28)</sup> However, the data revealed differences in how morphological traits related to tissue quality. Females tended to have more slender bones compared with males, which would be expected based on known sexually dimorphic growth patterns.<sup>(48)</sup> Female tibias also have a slightly larger mineralization, extending the observed relationship between morphology and composition in males. Although the overall relationship among Tt.Ar/Le, Ct.Ar/Tt.Ar, and ash content was similar for males and females, Ma.Ar proved to be a strong covariate for ash content in the path analysis for females but not males. This is consistent with dimorphic growth patterns after puberty, in which the endosteum switches from expansion to infilling for females. In males, the marrow space continues to expand in proportion to periosteal expansion. Prior work showed that females prone to stress fractures had more narrow tibias and thinner cortices compared with females that did not develop stress fracture.<sup>(8)</sup> Having slender bones plus thinner cortices may indicate that, for these individuals, there was a lack of infilling or lack of co-adaptation between periosteal and endosteal surface movements during growth.

*Summary*

The results of this study identified functional interactions among physical bone traits, suggesting that bone possesses important biological processes that co-adapt morphological and compositional traits so the set of traits results in a structure sufficiently stiff for daily activities. These results have important clinical implications because bone functionality and bone biology may be better understood based on knowledge of sets of traits rather than a single complex trait such as bone mass. Variation in the ability of bone to co-adapt traits would be expected to lead to under- and over-designed structures. The downside of co-adapting matrix composition is that increases in mineralization result in a more brittle and damageable material that would be expected to perform poorly under extreme load conditions. Thus, for more slender bones, reduced tissue ductility and toughness associated with greater ash content may increase the risk of fracturing from low cycle fatigue (e.g., military training) and overload (e.g., falling). Therefore, rather than using complex traits or a series of unrelated traits, clinical assessment of fracture risk may benefit from knowledge of sets of traits and the functional interactions among the traits.

## ACKNOWLEDGMENTS

The authors thank Haviva Goldman, PhD, and Mitchell B Schaffler, PhD, for suggestions in establishing the histological protocols. The authors thank the U.S. Department of Defense (DAMD17-01-1-0806) and the National Institutes of Health (AR44927) for support of this research. Samples were acquired through the Musculoskeletal Transplant Foundation (Edison, NJ, USA) and the National Disease Research Interchange (Philadelphia, PA, USA).

## REFERENCES

1. Albright F, Smith PH, Richardson AM 1941 Post-menopausal osteoporosis. Its clinical features. *JAMA* **116**:2465–2474.
2. Landin L, Nilsson BE 1983 Bone mineral content in children with fractures. *Clin Orthop Relat Res* **178**:292–296.
3. Chan GM, Hess M, Hollis J, Book LS 1984 Bone mineral status in childhood accidental fractures. *Am J Dis Child* **138**:569–570.
4. Milgrom C, Giladi M, Stein M, Kashtan H, Margulies JY, Chisin R, Steinberg R, Aharonson Z 1985 Stress fractures in military recruits. A prospective study showing an unusually high incidence. *J Bone Joint Surg Br* **67**:732–735.
5. Giladi M, Milgrom C, Simkin A, Stein M, Kashtan H, Margulies J, Rand N, Chisin R, Steinberg R, Aharonson Z, Kadem R, Frankel VH 1987 Stress fractures and tibial bone width. A risk factor. *J Bone Joint Surg Br* **69**:326–329.
6. Gilsanz V, Loro ML, Roe TF, Sayre J, Gilsanz R, Schulz EE 1995 Vertebral size in elderly women with osteoporosis. Mechanical implications and relationship to fractures. *J Clin Invest* **95**:2332–2337.
7. Crossley K, Bennell KL, Wrigley T, Oakes BW 1999 Ground reaction forces, bone characteristics, and tibial stress fracture in male runners. *Med Sci Sports Exerc* **31**:1088–1093.
8. Beck TJ, Ruff CB, Shaffer RA, Betsinger K, Trone DW, Brodine SK 2000 Stress fracture in military recruits: Gender differences in muscle and bone susceptibility factors. *Bone* **27**:437–444.
9. Duan Y, Seeman E, Turner CH 2001 The biomechanical basis of vertebral body fragility in men and women. *J Bone Miner Res* **16**:2276–2283.
10. Kiel DP, Hannan MT, Broe KE, Felson DT, Cupples LA 2001 Can metacarpal cortical area predict the occurrence of hip fracture in women and men over 3 decades of follow-up? Results from the Framingham Osteoporosis Study. *J Bone Miner Res* **16**:2260–2266.
11. Milgrom C, Giladi M, Simkin A, Rand N, Kedem R, Kashtan H, Stein M, Gomori M 1989 The area moment of inertia of the tibia: A risk factor for stress fractures. *J Biomech* **22**:1243–1248.
12. Beck TJ, Ruff CB, Mourtada FA, Shaffer RA, Maxwell-Williams K, Kao GL, Sartoris DJ, Brodine S 1996 Dual-energy X-ray absorptiometry derived structural geometry for stress fracture prediction in male U.S. Marine Corps recruits. *J Bone Miner Res* **11**:645–653.
13. Jepsen KJ, Pennington DE, Lee YL, Warman M, Nadeau J 2001 Bone brittleness varies with genetic background in A/J and C57BL/6J inbred mice. *J Bone Miner Res* **16**:1854–1862.
14. Jepsen KJ, Akkus OJ, Majeska RJ, Nadeau JH 2003 Hierarchical relationship between bone traits and mechanical properties in inbred mice. *Mamm Genome* **14**:97–104.
15. Jepsen KJ, Hu B, Tommasini SM, Courtland HW, Price C, Terranova CJ, Nadeau JH 2007 Genetic randomization reveals functional relationships among morphologic and tissue-quality traits that contribute to bone strength and fragility. *Mamm Genome* **18**:492–507.
16. Olson EC, Miller RL 1958 *Morphological Integration*. The University of Chicago Press, Chicago, IL, USA.
17. Currey JD 1979 Mechanical properties of bone tissues with greatly differing functions. *J Biomech* **12**:313–319.

18. Carrier D, Leon LR 1990 Skeletal growth and function in the California gull (*Larus californicus*). *J Zool* **222**:375–389.
19. Ferretti JL, Capozza RF, Mondelo N, Zanchetta JR 1993 Interrelationships between densitometric, geometric, and mechanical properties of rat femora: Inferences concerning mechanical regulation of bone modeling. *J Bone Miner Res* **8**:1389–1396.
20. Papadimitriou HM, Swartz SM, Kunz TH 1996 Ontogenetic and anatomic variation in mineralization of the wing skeleton of the Mexican free-tailed bat, *Tadarida brasiliensis*. *J Zool* **240**:411–426.
21. Thompson D 1961 *On Growth and Form*. Cambridge University Press, Cambridge, UK.
22. Sumner DR, Andriacchi TP 1996 Adaptation to differential loading: Comparison of growth-related changes in cross-sectional properties of the human femur and humerus. *Bone* **19**:121–126.
23. Moro M, van der Meulen MC, Kiratli BJ, Marcus R, Bachrach LK, Carter DR 1996 Body mass is the primary determinant of midfemoral bone acquisition during adolescent growth. *Bone* **19**:519–526.
24. Forwood MR, Bailey DA, Beck TJ, Mirwald RL, Baxter-Jones AD, Uusi-Rasi K 2004 Sexual dimorphism of the femoral neck during the adolescent growth spurt: A structural analysis. *Bone* **35**:973–981.
25. Currey JD 1984 Effects of differences in mineralization on the mechanical properties of bone. *Philos Trans R Soc Lond B Biol Sci* **304**:509–518.
26. Cheverud JM 1996 Developmental integration and the evolution of pleiotropy. *Am Zool* **36**:44–50.
27. Tommasini SM, Nasser P, Schaffler MB, Jepsen KJ 2005 Relationship between bone morphology and bone quality in male tibias: Implications for stress fracture risk. *J Bone Miner Res* **20**:1372–1380.
28. Tommasini SM, Nasser P, Jepsen KJ 2007 Sexual dimorphism affects tibia size and shape but not tissue-level mechanical properties. *Bone* **40**:498–505.
29. Ruff CB 2000 Body size, body shape, and long bone strength in modern humans. *J Hum Evol* **38**:269–290.
30. Currey JD, Alexander RMcN 1985 The thickness of the walls of tubular bones. *J Zool* **206**:453–468.
31. Gustafson MB, Martin RB, Gibson V, Storms DH, Stover SM, Gibeling J, Griffin L 1996 Calcium buffering is required to maintain bone stiffness in saline solution. *J Biomech* **29**:1191–1194.
32. Nadai A 1950 *Theory of Flow and Fracture of Solids*. Engineering Societies Monographs. McGraw-Hill, New York, NY, USA.
33. Burstein AH, Currey JD, Frankel VH, Reilly DT 1972 The ultimate properties of bone tissue: The effects of yielding. *J Biomech* **5**:35–44.
34. Jepsen KJ, Davy DT 1997 Comparison of damage accumulation measures in human cortical bone. *J Biomech* **30**:891–894.
35. Wright S 1921 Correlation and causation. *J Agric Res* **20**:557–585.
36. Price CP, Herman BC, Lufkin T, Goldman HM, Jepsen KJ 2005 Genetic variation in bone growth patterns defines adult mouse bone fragility. *J Bone Miner Res* **20**:1983–1991.
37. Grace JB 2006 *Structural Equation Modeling and Natural Systems*. Cambridge University Press, Cambridge, UK.
38. Stieger JH, Lind JM 1980 Statistically Based Tests for the Number of Common Factors Annual Meeting of the Psychometric Society, Iowa City, IA, USA, May 1980.
39. MacCallum RC, Hong S 1997 Power analysis in covariance structural modeling using GFI and AGFI. *Multivariate Behav Res* **32**:193–210.
40. Tommasini SM, Morgan TG, van der Meulen M, Jepsen KJ 2005 Genetic variation in structure-function relationships for the inbred mouse lumbar vertebral body. *J Bone Miner Res* **20**:817–827.
41. Brear K, Currey JD, Pond CM 1990 Ontogenetic changes in the mechanical properties of the femur of the polar bear *Ursus maritimus*. *J Zool* **222**:49–58.
42. Carrier DR 1983 Postnatal ontogeny of the musculo-skeletal system in the Black-tailed jack rabbit. *J Zool* **201**:27–55.
43. Heinrich R 1999 Ontogenetic changes in mineralization and bone geometry in the femur of muskoxen (*Ovibos moschatus*). *J Zool* **247**:215–223.
44. Martin RB, Ishida J 1989 The relative effects of collagen fiber orientation, porosity, density, and mineralization on bone strength. *J Biomech* **22**:419–426.
45. Currey JD 1988 The effect of porosity and mineral content on the Young's modulus of elasticity of compact bone. *J Biomech* **21**:131–139.
46. Ural A, Vashishth D 2006 Interactions between microstructural and geometrical adaptation in human cortical bone. *J Orthop Res* **24**:1489–1498.
47. Bonadio J, Jepsen KJ, Mansoura MK, Jaenisch R, Kuhn JL, Goldstein SA 1993 A murine skeletal adaptation that significantly increases cortical bone mechanical properties. Implications for human skeletal fragility. *J Clin Invest* **92**:1697–1705.
48. Garn S 1970 *The Earlier Gain and the Later Loss of Cortical Bone*. Charles C Thomas, Springfield, IL, USA.
49. Sinervo B, Svensson E 2002 Correlational selection and the evolution of genomic architecture. *Heredity* **89**:329–338.
50. Nadeau JH, Burrage LC, Restivo J, Pao YH, Churchill G, Hoit BD 2003 Pleiotropy, homeostasis, and functional networks based on assays of cardiovascular traits in genetically randomized populations. *Genome Res* **13**:2082–2091.
51. Duan Y, Parfitt A, Seeman E 1999 Vertebral bone mass, size, and volumetric density in women with spinal fractures. *J Bone Miner Res* **14**:1796–1802.
52. Skaggs DL, Loro ML, Pitukcheewanont P, Tolo V, Gilsanz V 2001 Increased body weight and decreased radial cross-sectional dimensions in girls with forearm fractures. *J Bone Miner Res* **16**:1337–1342.

Address reprint requests to:  
 Karl J Jepsen, PhD  
 Department of Orthopaedics  
 Mount Sinai School of Medicine  
 Box 1188, One Gustave L. Levy Place  
 New York, NY 10029, USA  
 E-mail: karl.jepsen@mssm.edu

Received in original form June 22, 2007; revised form September 10, 2007; accepted October 3, 2007.